VAK 2024 MODERN ASTRONOMY: FROM THE EARLY UNIVERSE TO EXOPLANETS AND BLACK HOLES 300 years Russian Academy of Sciences

Photospheric disturbances and acoustic sources of the helioseismic "circular" X1.5 flare of May 10, 2022

I. Sharykin and I. Zimovets

Space Research Institute of the Russian Academy of Sciences, Profsoyuznaya Str. 84/32, Moscow, 117997 Russia

Abstract. This paper is devoted to the analysis of the energy release of the X1.5-class solar flare that occurred on May 10, 2022, during which the powerful helioseismic response ("sunquake") was observed. An additional feature is the fact that this powerful sunquake was generated in the NOAA active region 13006 of Hale class $\beta\delta$, whereas earlier it was shown that the strongest helioseismic disturbances are generated in the sunspot groups with the most complex Hale class of $\beta\gamma\delta$. We analyze magnetic fields and photospheric perturbations basing on the Helioseismic and Magnetic Imager (HMI) data. Analysis of the distribution of acoustic sources and photospheric perturbations reveals a ring geometry in the form of a chain of sources roughly corresponding to the geometry of flare ribbons. The photospheric perturbations developed in two regions near the magnetic field polarity inversion line (PIL) and corresponded to two series of hard X-ray bursts seen in the KONUS/WIND data. We extrapolated the coronal magnetic field from the HMI vector magnetograms within the framework of the nonlinear force-free field (NLFFF) approximation. The geometry of the "dome with a spine" type was revealed. The regions of the photospheric perturbations approximately corresponded to the base of the dome. In this work we also briefly discuss penumbral decay and the flare dynamics of the observed δ-spot. The data obtained vividly show the local features of the magnetic fields in a relatively morphologically simple active region, where the conditions for the powerful helioseismic response during the solar flare arose. The paper also discusses the morphological properties of the active region with similar properties of the most helioseismically active regions of the 24th cycle.

Keywords: Sun: sunquakes, solar flares, active regions, magnetic fields, sunspots

DOI: 10.26119/VAK2024.116

1 Introduction

The paper is devoted to the case-study of the helioseismically active X1.5 solar flare (its helioseismicity was firstly discovered and discussed in Kosovichev et al. 2023), briefly described in the abstract. Helioseismic solar flare impacts are reffered as sunquakes and seen as concentric ripples in photospheric Dopplergrams running from compact regions connected with the sites of the flare photospheric energy release (see review of Kosovichev 2015). The catalog of helioseismically active solar flares of the 24th solar activity cycle (Sharykin & Kosovichev 2020) shows that every fifth M and X class flare or every second flare with a photospheric perturbation is characterized by the appearance of the helioseismic waves. Thus, this phenomenon is not rare and is characterised by particular interest for studying complex flare energy release.

There is still no clear understanding of the nature of sunquakes. There are a few hypothesis of the sunquake generation (e.g., see introduction in Sharykin & Kosovichev 2020): perturbations induced by nonthermal particles (electrons or ions), changing magnetic field or dissipation of electric currents. It is also possible to assume the simultaneous contribution of various mechanisms, the effectiveness of which may change as the flare develops. Today we do not know the exact cause of sunquakes and need additional research and statistical work.

One of the ways to study the physics of sunquakes is to search for unique events with special morphological properties that may indicate the necessary conditions for the occurrence of heliosesmic perturbations. This article considers such a solar flare. And the main goal of this work is to find specific features (local or global) of the active region producing solar flares accompanied by sunquakes.

2 The analysed solar flare and the used observational data

The considered sunquake was generated in the NOAA active region 13006 of Hale class $\beta\delta$ and McIntosh class Cso. Earlier in the statistical work of Sharykin & Kosovichev (2020) it was shown that the strongest helioseismic disturbances are generated in the sunspot groups with the most complex Hale class $\beta\gamma\delta$. And there were no heliosesmically active solar flares in the active regions with such "simple" (in comparison with Cso) McIntoch class during the 24th solar cycle. For example, the typical classes were: Dkc => Ekc (NOAA 12673, 5–7 September 2017); Fkc => Ekc => Fhc (NOAA 11515, 4–7 July 2012); Fkc (NOAA 12192, 20–26 October 2014); Dkc (NOAA 11429, 5–7 March 2012).

The relative global simplicity of the considered active region (compared to other ARs causing sunquake flares) with the large energy of the considered sunquake event

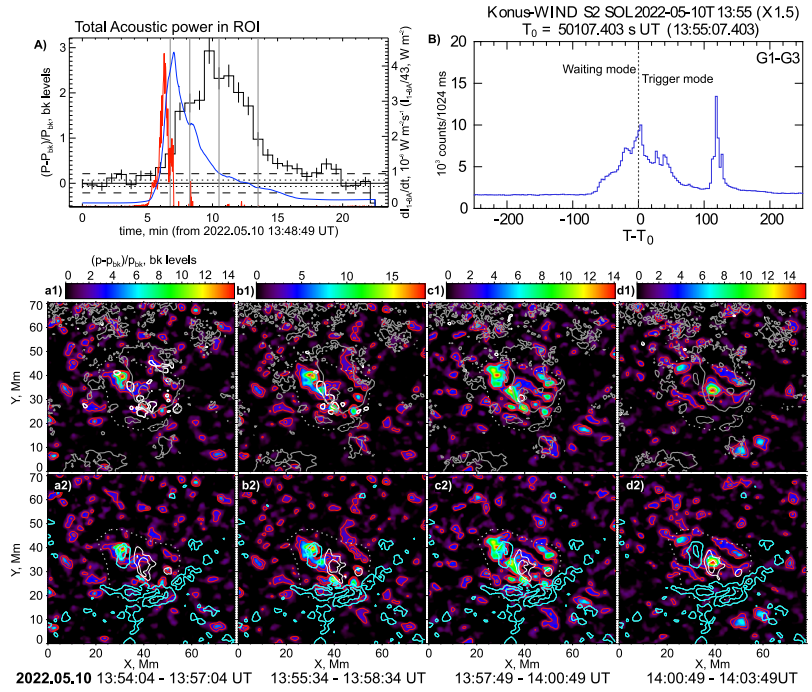

Fig. 1. Panel A: GOES 1–8 Å lightcurve (blue) and its time derivative (red); Normalized acoustic power with errors in units of background levels (black histogram). Vertical lines in A show positions of the time intervals used to generate acoustic maps in (a–d) panels. Horizontal lines show 1 and 3 sigma levels around zero acoustic power. KONUS/WIND HXR lightcurve (G1-G3 channels) is shown in panel B. Panels (a1–d1): acoustic power maps (background rainbow colored maps) with overlayed white contours (300 m/s) of LOS Doppler velocity perturbations and PIL (grey lines). Panels (a2–d2) also contain acoustic power maps, but with the overlayed contours of the magnetic field vertical component (cyan – negative, white – positive).

and X GOES flare class gives us a chance to find AR peculiarities responsible for strong sunquakes.

In this work we mostly consider line-of-sight Dopplergrams (45 seconds cadence) and vector magnetograms (Hoeksema et al. 2014) with 720 seconds cadence from the Helioseismic and Magnetic Imager (HMI, Scherrer et al. 2012) onboard the Solar Dynamics Observatory.

3 Properties of the flare phototspheric disturbances

Analysis of the sunquake event and the corresponding photospheric perturbations is shown in Fig.1. We used acoustic holography method and reconstructed the dynamics of the acoustic helioseismic power (A) in the region of interest covering the flare site

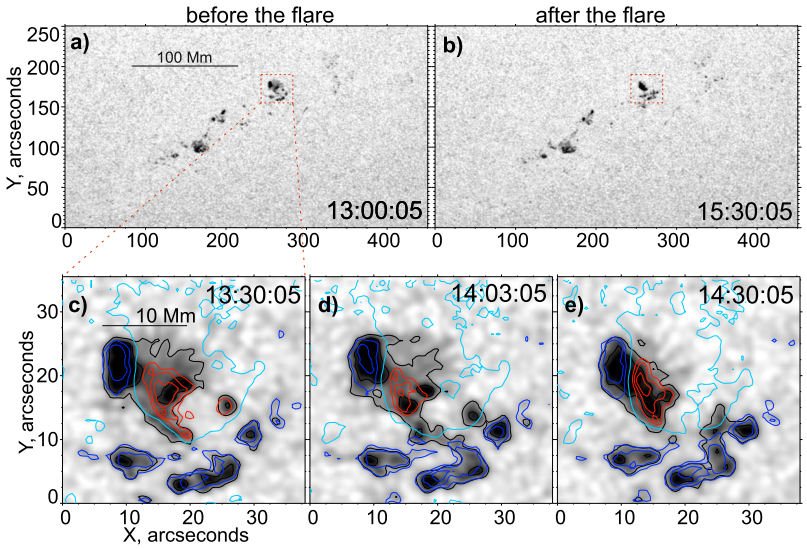

Fig. 2. HMI intensity maps of the NOAA AR 13006 for time instants before and after the flare are compared in panels (a) and (b). ROI corresponding to the main flare energy release is shown by the dashed red rectangular box in (a). Panels (c–d) present dynamics of the HMI intensity maps, LOS magnetic field for negative (blue) and positive (red) directions, and PIL (cyan) for the selected ROI.

(ROI in panels (a–d) marked by dashed contour). The time sequence of 3-minute averaged acoustic maps (a–d) shows that photospheric disturbances and acoustic sources are located along the LIP, forming a quasi-ring "chain" of impacts.

During the flare there were two HXR pulses (Fig.1–B) according to the KONUS/WIND data (18–300 keV): gradual ($\sim$ 180 s) and the impulsive ($\sim$ 30 s). These two bursts have corresponding non-spatial photospheric disturbances in the PIL (white contours of panels (a1) and (b1)). The strongest acoustic sources were located in the sunspots (a2–d2) and in the interspot PIL regions (b2–c2).

4 Dynamics of the morphology of sunspots and magnetic fields

We found significant flare-associated changes in the morphology of the leading δ-sunspot. General view of the studied active region before and after the flare is shown in Fig.2(a, b) (HMI continuum intensity maps with 45-sec cadence). The ROI around the photospheric perturbations is marked by the rectangular dashed box. Note that the asymmetric penumbra experienced decay and the leading sunspot became rather compact ($\sim$ 10 Mm) penumbra-less sunspot.

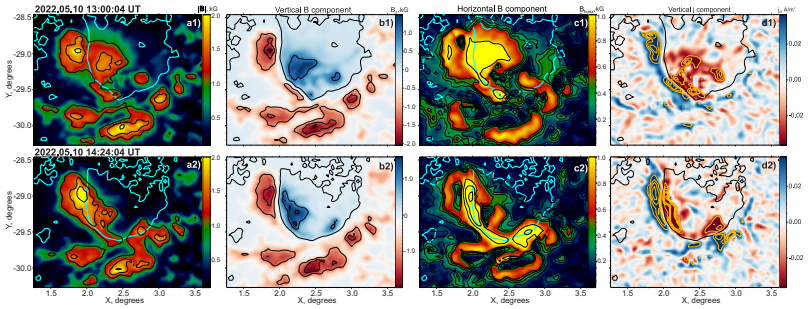

Fig. 3. The following maps deduced from HMI vector magnetograms are shown: Absolute value of magnetic field (a); Vertical magnetic component (b); Horizontal component (c); Vertical electric current density (d). PIL is shown by black (b, d) and cyan (a, c) curves. Regions of enhanced values of the magnetic field components and electric current are highlighted by contours with different levels (black in (a–c) and orange in (d)).

Penumbra decay and corresponding dynamics of the LOS magnetic field is clearly shown by three frames in Fig.3(c–e). One can note that the observed δ-spot (two umbras of opposite polarities in the common penumbra) experienced compactification and became δ-spot with a single umbra (we do not separate two initial umbras). These changes are connected with the magnetic field restructuring around the δ-spot, where the flare energy release took place. Magnetic field changes were detected in all three magnetic field components. The most dramatic changes were: 1) “compression” of the magnetic field of the δ-spot (a1–a2) and formation of a single umbra δ-spot with the PIL inside it and degradated penumbra; 2) significant changes in the distribution of the horizontal magnetic field (c1–c2) highlighting penumbral decay and growth of the horizontal component value at the PIL; 3) restructuring of the electric current system (d1–d2).

The non-linear force free modelling (NLFFF, based on the optimization method in approach of Rudenko & Myshyakov 2009) of the coronal magnetic field reveals a compact dome structure with a spine (yellow lines in Fig. 4), covering the flare δ-spot region where we observed the sunquake event. An extremely sheared current-carrying magnetic structure lying along the PIL is shown by red lines.

5 Concluding remarks

The performed analysis of the helioseismic X1.5 solar flare with the powerful sunquake in the $Cso\ \beta\delta$ active region revealed that the spatial distribution of the acoustic sources and photospheric impacts were associated with the dome-spine magnetic field topology located around the δ-spot. We found significant magnetic field changes with

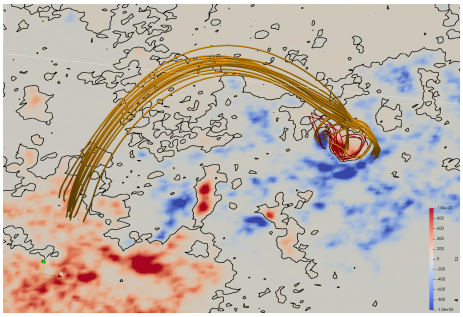

Fig. 4. Topology of the coronal magnetic field lines (based on the NLFFF reconstruction) around the flare region. The blue-red background image shows the vertical magnetic field map. The black curve is the PIL. Yellow lines mark magnetic field lines forming the dome and spine. Red lines mark the twisted magnetic structure lying along the PIL and covered by the dome.

penumbral decay during the flare with restructuring electric current system. This example of the powerful sunquake in the rather "simple" (from the point of view of McIntosh classification) active region shows that we need a dynamic δ-sunspot for efficient helioseismicity. However, this short study did not give us an answer to the question of which agent directly disturbed the photosphere. It is possible that the observed dynamics of the δ-spot magnetic field leads to effective acceleration and formation of electron (or ion) beams that effectively disturb the lower solar atmosphere. However, other mechanisms (dissipation of electric current or pulsed magnetic forces) cannot be ignored. To obtain clearer results about the nature of sounquakes, we need more case-studies, statistics and theoretical/modeling research. We believe that the conditions favorable for sunquakes in the analyzed active region discussed in this paper can provide direction for future observational and theoretical studies.

Acknowledgements. We thank the many team members who contributed to the success of the SDO mission and, especially, the HMI instrument.

Funding

The work was supported by the Russian Science Foundation grant No. 23-72-30002.

References

Hoeksema J.T., Liu Y., Hayashi K., et al., 2014, Solar Physics, 289, 9, p. 3483
Kosovichev A.G., Sadykov V.M., Stefan J.T., 2023, Astrophysical Journal, 958, 2, id. 160
Kosovichev A.G., 2015, Extraterrestrial Seismology, ed. V. Tong & R. García, p. 306
Rudenko G.V. and Myshyakov I.I., 2009, Solar Physics, 257, 2, p. 287
Sharykin I.N. and Kosovichev A.G., 2020, Astrophysical Journal, 895, 1, id. 76
Scherrer P.H., Schou J., Bush R.I., et al., 2012, Solar Physics, 275, 1-2, p. 207